Int. J. Electrochem. Sci., 11 **(2016)** 815 - 835

International Journal of
ELECTROCHEMICAL
SCIENCE
www.electrochemsci.org

Utilization of New Anionic Polymeric Surfactants for Corrosion Inhibition Enhancement in Petroleum Industries

M. R. Noor El-Din[*], *R.K. Farag, O.E. Elazbawy*

Egyptian Petroleum Research Institute, 1 Ahmed El- Zomor St., Nasr City, 11727, Cairo, Egypt.
[*]E-mail: mrned04@gmail.com

Received: 12 May 2015 / *Accepted:* 12 September 2015 / *Published:* 1 December 2015

In this work, 2-acrylamido-2-methylpropane sulfonic acid-CO-lauryl acrylate copolymer is used in the synthesis of three new anionic polymeric surfactants for use in corrosion protection of petroleum pipelines composed of carbon steel alloy. The corrosion inhibition performance of the prepared inhibitors was measured using weight loss and electrochemical methods in 1M HCL. The morphology of untreated and treated carbon steel surfaces was studied by scanning electron microscopy (SEM). Also, the thermodynamic properties as well as surface tension were investigated for the prepared inhibitors. Adsorption phenomena for the prepared surfactants on the carbon steel alloy were found to obey Langmuir's law. The quantum chemical parameters as highest occupied molecular orbital (E_{HOMO}), lowest unoccupied molecular orbital (E_{LUMO}) and energy gap (ΔE) were computed for the prepared inhibitors and it was found that LP3 had higher efficiency than others.

Keywords: Polymeric surfactants; Corrosion inhibitors; Carbon steel alloy; Polarization; Quantum chemical parameters; Electrochemical calculation

1. INTRODUCTION

It is a fact that, corrosion of metallic equipment's has great negative effect on the investment of petroleum sector [1]. Acidic solutions, which mainly caused the corrosion of petroleum equipment's, one of the most used in petroleum applications as in pickling, petroleum pipelines cleaning and acid de-scaling [2]. Commonly hydrochloric and sulphuric acids are the main types of acidic solutions causing the corrosion of the metallic surfaces especially that consists of iron and its alloys. The corrosion is minimized by different chemicals as inhibitors that based on nitrogen-, sulphur-, and/or oxygen-containing organic compounds [3]. However, sulphur-, nitrogen-, and/or oxygen-containing organic compounds are preferred for H_2SO_4 and HCl media. The efficiency of the corrosion inhibitors depends on the absorptivity of the inhibitors on the corroded surface, which is currently depends on its morphology and the metal surface state, the chemical constituent of the used inhibitor and the type of acidic solution [4]. Using the surfactants as corrosion inhibitors seems to be advantages for their low cost and toxicity in addition to their production procedure is known to be very simple [1]. The corrosion resistance of any metallic surface is affected the adsorption of the inhibitor on the surface [5]. One of the most famous types of surfactants used as corrosion inhibitors is the ionic surfactant. This type of surfactant is used as corrosion inhibitors for protection both of iron [6], copper [7], aluminium [8] and others [9] in different corroding media. Recently, the effect of the molecular structure of the inhibitors (organic or surfactant type) on its adsorption efficiency on the surface metal was investigated by quantum-chemistry calculations. This investigation is used to predict the efficiency of inhibitors through its reaction mechanism before application step [10]. In this research, a new type of anionic polymeric surfactant was synthesized and evaluated as corrosion inhibitors for carbon steel alloy in 1M HCl solution. The evaluation procedure was done using both of weight loss and electrochemical techniques. Also, the correlations between the inhibition efficiency of the prepared anionic inhibitors and some quantum parameters were studied.

2. EXPERIMENTAL

2.1. Materials

Analytical grades of lauryl acrylate (donated as L), and 2-acrylamido-2-methylpropane sulfonic acid (donated as P) were supplied by Sigma–Aldrich Co., UK. Technical grades of dimethylformamide (DMF), Tetrahydrofuran (THF) and ethanol were obtained from Fluka, Germany. Benzoyl peroxide (99% purity) as initiator was delivered from Alderich chemical Co. A technical grade of ammonium hydroxide was acquired from Sidi-Kerier Petrochemicals Co. (SIDPEC), Alexandria, Egypt.

2.2. Synthesis of inhibitors

2.2.1. Synthesis of (2-acrylamido-2-methylpropane sulfonic acid / lauryl acrylate) copolymer

In this step, a typical polymerization batch of (0.15, 0.1 and 0.5) moles of lauryl acrylate and (0.85, 0.90 and 0.95) moles of 2-acrylamido-2-methylpropane sulfonic acid monomers were firstly dissolved in 100 ml of dimethylformamide in a reactor having a capacity of 100 ml equipped with a condenser under nitrogen gas in a water bath at 70ºC ± 0.1ºC (working temperature). 0.01% (weight ratio with respect to the monomers) of benzoyl peroxide as initiator was added to the monomers solution at working temperature. The ingredient mixture was purged with N_2 gas for 30 minutes, and then it was kept for another 120 minutes 70ºC ± 0.1ºC. The polymerization reaction was stopped and the cooled copolymers were purified by extraction from DMF using a mixed solvent of DMF/ ethanol (70/90wt./wt.), respectively. The extract was washed and dried until constant weight [11].

2.2.2. Preparation of [(2-acrylamido-2-methylpropane sulfonic acid/lauryl acrylate) copolymer] ammonium salt

In 250 ml round bottle equipped with magnetic stirrer, (9.8, 8.3and 7.3)$\times 10^{-4}$ mole of each previously prepared copolymer was neutralized by ammonium hydroxide solution (29% concentration) using ADWA PH-meter model AD110, Germany. The reaction scheme of the prepared inhibitors is shown in Figure 1.

2.3. Characterization of the synthesized inhibitors

2.3.1. Fourier transform infrared spectroscopy (FTIR)

The chemical structure of the prepared inhibitors was confirmed using FTIR spectrometer of model type Thermo Fisher Scientific (USA). The sample was compressed into a desk after mixing with KBr.

2.3.2. Gel permeation chromatography (GPC)

The molecular weights of the synthesized inhibitors were performed at 40 ^{o}C using GPC-Water 2410, with a refractive index detector using 4 columns styragel HR THF 7.8 x 300 mm, equipped with a water 515 HPLC pump. Tetrahydrofuran (THF) and water were used as mobile phase at a flow rate of 1 ml/min. Aliquots (1 ml) of each sample were diluted with an appropriate amount of THF or water and shaken vigorously, and then it was filtered and injected into the GPC for analysis.

2.4. Corrosion inhibitors evaluation

2.4.1. Surface tension measurements (γ)

The surface tension (γ) for the prepared anionic polymeric surfactants was measured at 25^{o}C using De-Noüy Tensiometer (Model Kruss-K6), Germany by using a platinum ring technique. The surface tension was measured for each surfactant for three times within three minutes interval between each reading [12].

A relation between surface tension (γ) and the logarithm of inhibitors concentration (lnC) was plotted and the *cmc* for each inhibitor was detected from the abrupt change in the slope of its plots. Maximum surface excess concentration (Γ_{max}), the minimum surface area per surfactant (A_{min}) was determined from the slope of the curve of (γ) versus (ln C). Also, thermodynamics parameters of adsorption and micellization Gibbs free energies such as; Gibbs free energy of adsorption (ΔG_{ads}) and micellization, (ΔG_{mic}) for the prepared polymers were calculated by utilization of Gibb's adsorption equations [13].

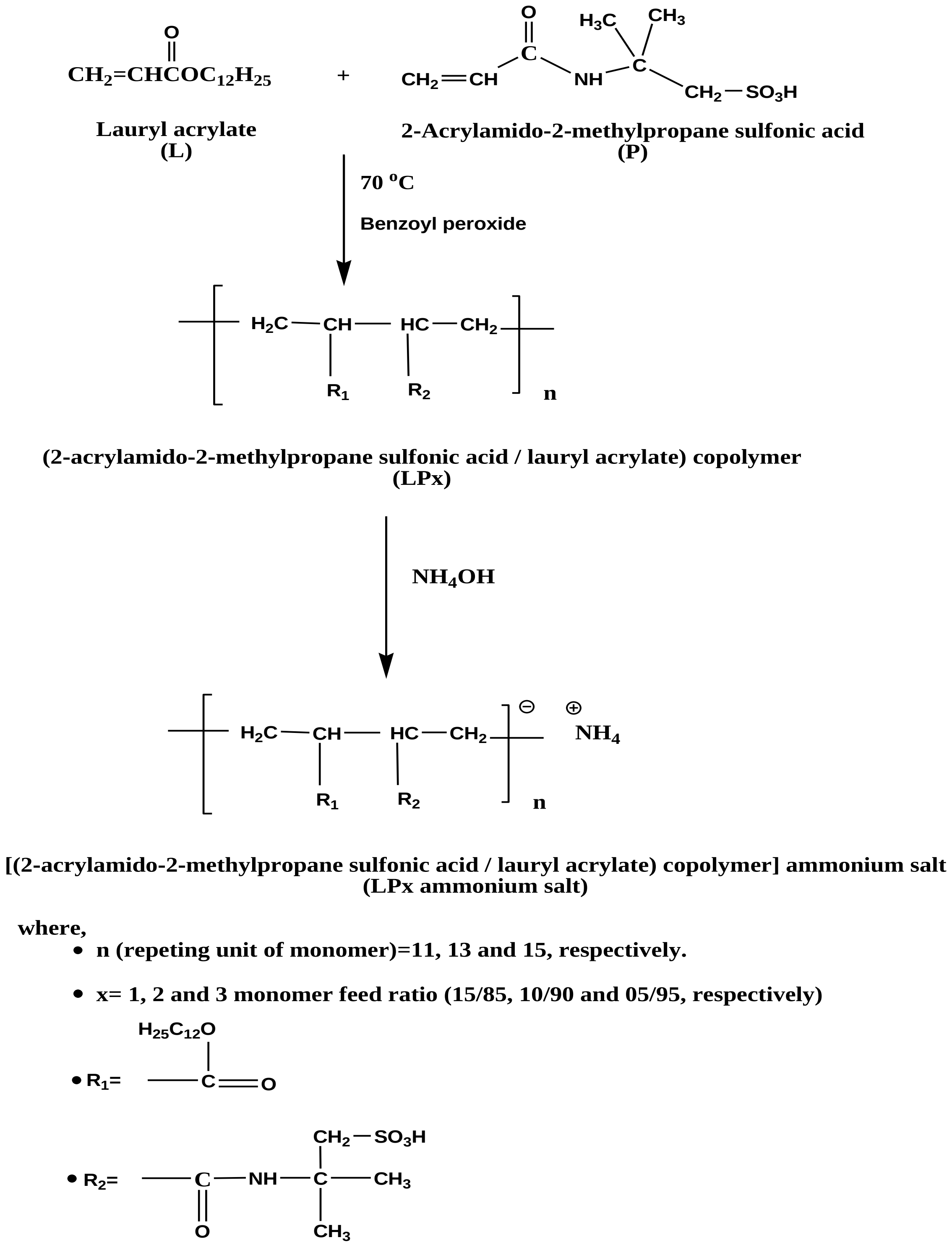

Figure 1. Chemical structure of the prepared inhibitors.

2.4.2. Electrochemical measurements

In this step, a carbon steel working electrode consists of: 0.07 % C, 0.24 % Si, 1.35 % Mn, 0.017 % P, 0.045% Sn, and the remainder Fe (wt%) was used. The sample of each specimen of steel was mechanically pretreated before testing by grinding using emery paper of grades 400, 600, 800 and

1,000. The electrode was washed with acetone and distilled water. Finally, the tested electrode was putted in dissector for drying. The electrochemical measurements were performed by Volta lab 40 (Tacussel-Radiometer PGZ301) potentiostate and controlled by Tacussel corrosion analysis software model (Volta-master 4) under static condition. The used corrosion cell used consists of three electrodes namely; 1) working electrode, 2) reference electrode was a saturated calomel electrode (SCE) and 3) auxiliary electrode (platinum type) was used, while, all the given potentials were referred to the reference electrode [14]. Potentiodynamic polarization plots were obtained by varying the potential electrode automatically (from -800 to -200 mV vs. SCE) at open circuit potential with scan rate 2 mV s^{-1}.

EIS measurements were carried out in a frequency range of 100 kHz to 10 mHz with amplitude of 4 mV peak-to-peak using signals at open circuit potential.

2.4.3. Weight loss measurements

Carbon steel sheets having dimensions of 7.0 × 2.0 × 0.3 cm were treated as mentioned previously in step (4.2). The specimens were immersed in 1M HCl solution as a blank (without inhibitors) and 1M HCl solution contain 20-100 ppm of the prepared surfactant for 24h at 303K respectively. Then, the steel were rinsed thoroughly with bi-distilled water, dried and weighted for accurate weight determining. The calculation of the average weight loss (ΔW, mg) was determined as follows [1]: -

$$\Delta W = W_1 - W_2 \qquad [1]$$

where, W_1 and W_2 are the average weights of steel sample before and after exposure to the used acidic media, respectively [15].

2.4.4. Surface Morphology Studies

The scanning electron microscopy (SEM) of model type JEOL 5410, JEOL, Japan was used to detect the surface morphology of the uncorroded sample. The surfaces of blank and treated sheet panel were also studied after immersing the sample in 1M HCl without and with of 100 ppm of each surfactant for 24 hours.

2.4.5. Quantum chemical study

The quantum chemical equipment's for the prepared polymers were calculated based on MINDO3 semi-empirical method using the Unrestricted HartreeFock (UHF) levels which are implemented in Hyperchem 8.0. The molecule 2D sketch was obtained by ISIS Draw 2.1.4. The calculation of other parameters namely; log P (hydrophobic parameter), polarizability and hydration energy were carried out by the QSAR method obtained from the optimized geometry [16].

3. RESULTS AND DISCUSSION

3.1. Characterization of the prepared 2-acrylamido-2-methylpropane sulfonic acid- CO-lauryl acrylate copolymer, ammonium salt

The prepared polymeric inhibitors structure (LP1, LP2 and LP3) was confirmed using both of FT-IR and gel permeation chromatography (GPC) techniques are shown as follows: -

3.1.1. Fourier transform-infrared spectroscopic and Gel permeation chromatography

The chemical structure of the prepared inhibitors (LP1, LP2 and LP3) was confirmed by Fourier transform-infrared spectroscopy (FT-IR) as shown in Figures 2(a-c), respectively. From Figure 2a, the FTIR spectrum of LP1 as a representative sample, shows characteristic absorption bands at 2,926 and 2,855 cm $^{-1}$ which assigned for stretching vibration of the aliphatic C-H bond. On the other hand, the peaks at 1,750 cm^{-1} assigned for stretching vibration of the C=O and the peaks at 1,143 cm^{-1} assigned for stretching of C-O. Also, the band of 1300 cm^{-1} assigned for asymmetric stretching S=O bond, the band of 650 cm^{-1} assigned for symmetric stretching S-O bond and 3,435 cm^{-1} assigned for stretching of -NH. Also, The disappearance of (C=C) band at 1,620 cm^{-1} confirms the completion of the polymerization reaction [17]. GPC results showed that the M_n values of LP1, LP2 and LP3 were 5,120, 5,970 and 6,830 Daltons, respectively (Table 1). The difference in the average molecular weight is attributes to the presence percentage of (P) monomer in the prepared polymeric inhibitors. As increasing the percentage of (P) monomer, both of the molecular weight and the solubility of inhibitor increases.

3.2. Evaluation of the synthesized inhibitors

3.2.1. Surface active and thermodynamic properties of the prepared inhibitors

The surface active parameters as critical micelle concentration (*cmc*), surface tension at critical cmc (γ_{cmc}), the maximum surface pressure (π_{cmc}), the maximum surface excess concentration

(Γ_{max}), and minimum area per molecule at solution-air interface (A_{min}) are illustrated in Table 1 and shown in Figure 3. Commonly, the results in Table 1 indicate that; 1) Using different monomer feed ratios (R_1/R_2) produces inhibitors having variable surface active and thermodynamics parameters 2) By increasing the content of R_2 (hydrophilic moiety part), the molecular weight of the resultant surfactant increases and 3) By increasing the molecular weight of the surfactant, its cmc *and* γ_{cmc} decrease, while its of π_{cmc} increase. In any case, the results show that the value of the surface tension (γ_{cmc}) of the prepared inhibitors decreases as its molecular weight increases, whereas, γ_{cmc} values are 46.1, 40.5 and 35.5 mNm^{-1} for LP1, LP2and LP3 and their M_n are 5,120, 5,970 and 6,830 Daltons, respectively.

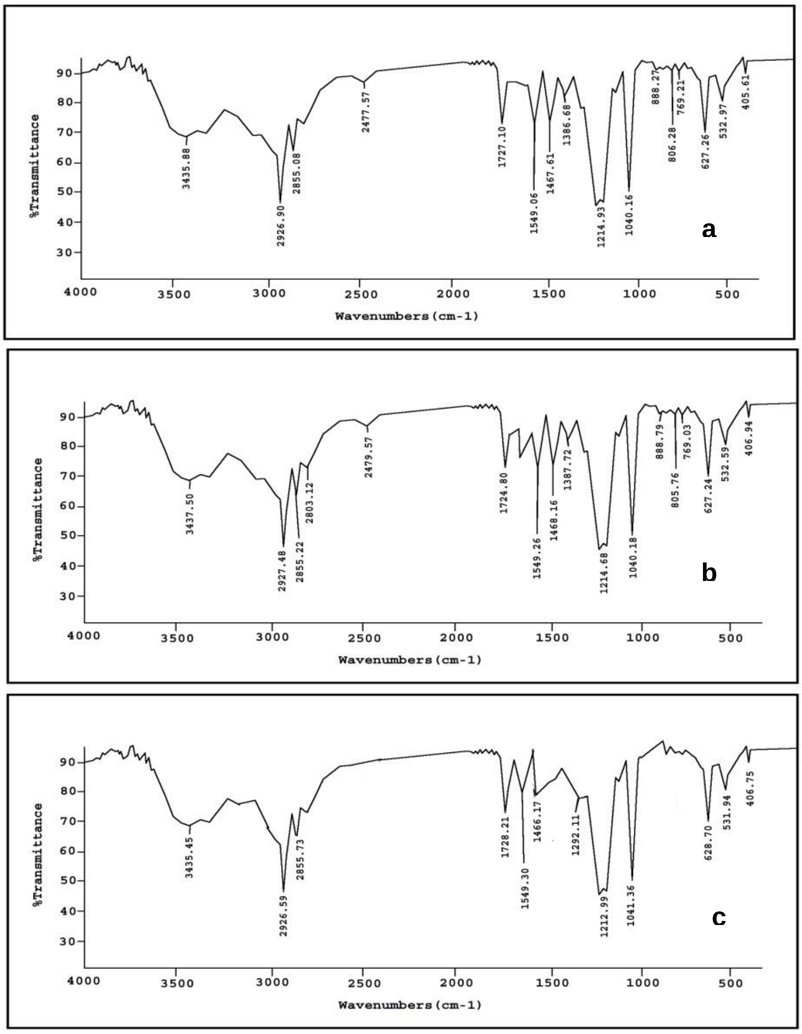

Figure 2. FT-IR spectra of a) LP1, b) LP2 and c) LP3.

Table 1. Surface active properties and thermodynamic parameters of the prepared inhibitors

Surfactant	***cmc**, mol dm^{-3}×10^{-4}**	**γ_{cmc}*, mNm^{-1}**	**π_{cmc}**, mNm^{-1}**	**Γ_{max}**, mol/cm^{-2} ×10^{10}**	**A_{min}**, nm^2/ molecule**	**ΔG_{mic}**, kJ /mol**	**ΔG_{ad}**, kJ /mol**	**M_n, Daltons**
LP1	2.441	46.1	21.92	2.34	73.00	-20.60	-21.46	5,120
LP2	2.094	40.5	27.50	2.34	70.87	-20.98	-22.10	5,970
LP3	1.627	35.5	32.50	2.77	59.89	-21.61	-22.99	6,830

***:** Precession of tensiometer

******: Precession of excel software.

This may be explained by that the increase in the molecular weight of the surfactant show an increase in the number of the heteroatoms in the repeating units of (R_1 and R_2) as shown in Figure 1. However, the adsorption power of the inhibitors on the surface metal is considered as a net result of the actions of both R_1 (hydrophobic moiety) and R_2 hydrophilic moiety). The increase of R_2 will increase the electrostatic attraction between the charge of metal surface and the long pair of the molecule itself [18]. Also, Γ_{max} and A_{min} was affected by the chemical structure and the percentage of R_2 in the prepared inhibitors, whereas, with the increase of the inhibitor molecular weight, Γ_{max} value increases and A_{min} value decreases. As expected, as the value of molecular weight of the prepared inhibitor increases is a result of increase in number of R_2 moiety in the repeating unit so, Γ_{max} increase. The data presented in Table 1 showed that by decreasing the hydrophilic moiety (R_2) of surfactant molecules, the Γ_{max} decrease. This means that the possibility of polymer to become more soluble in water would be decrease. As a result of the decreasing of the Γ_{max} values, the area at the interface for each surfactant molecules will be increased [19]. On the other hand, A_{min} value decreases with the increase in the value of molecular weight as a result of decrease in the area occupied on the metal surface [20]. This area controlled by the competition between Vander Waals forces among aliphatic chains and repulsive interaction (electrostatic or hydration forces) between polar head group impact on the resulting value of A_{min}. [21]. That is the reason of decreasing the A_{min} value of LP3 than those of LP1 and LP2. The standard free energies of micellization (ΔG_{mic}) and adsorption ($\Delta G_{ad.}$) of the synthesized surfactants were calculated and the results listed in Table 1. From the obtained data of ΔG_{mic}, it can be assumed that the micellization process is spontaneous because $\Delta G_{mic} < 0$. Generally, the ΔG_{ads} is lower than ΔG_{mic} values. This indicates that, these polymers favor adsorption more than micellization. Obviously, this favourability of adsorption is attributed to interaction forces between hydrophobic chains and the polar medium and the minimum value of the polymer molecules situated at the air/water interface. Thus, the maximum $-\Delta G_{ad}$ (-20.33 Kj/mol) was obtained by (LP3) which exhibited the maximum inhibition efficiency.

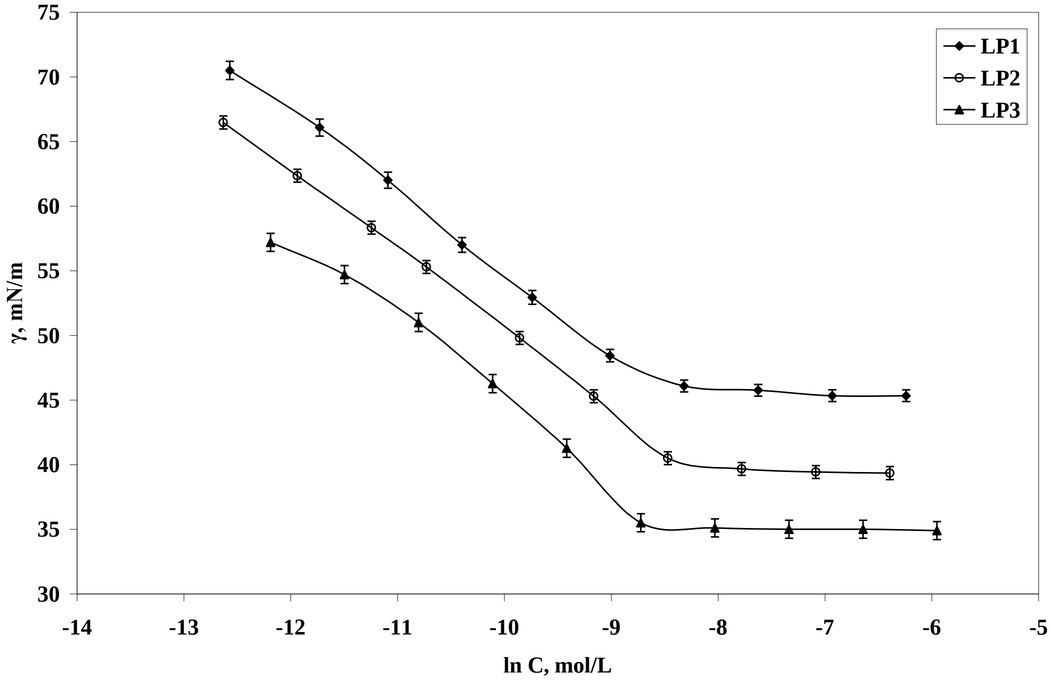

Figure 3. γ –ln C adsorption isotherm for prepared cationic surfactants (using three repeating reading obtained and excel software).

3.2.2. Potentiodynamic polarization measurements

The polarization plots for carbon steel in 1M HCl with and without different concentrations of the prepared inhibitors ranging from 20-100 ppm at 303 K are shown in Figures 4-6. The parameters of potentiodynamic polarization are; potential for corrosion (E_{corr}), current density values (i_{corr}), anodic Tafel slope (β_a), cathodic Tafel slope (β_c), and the inhibition efficiency (I%) were determined and listed in Table 2. The inhibition efficiency (I %) and the corrosion rate (C.R.) is calculated from polarization curves according to the relations given below: -

$$I\% = \frac{icorr(uninh) - icorr(inh)}{icorr(uninh)} \times 100 \qquad [2]$$

Where, $i_{corr(uninh)}$ and $i_{corr(inh)}$ are uninhibited and inhibited corrosion current densities, respectively.

$$C.R.(mpy) = \frac{0.13\ icorr\ (E.W.)}{d} \qquad [3]$$

Where, mpy, i_{corr}, d and E.W. are milli inches per year, the corrosion current densities, density of the corroding species (g/cm^3), and the equivalent weight of the corroding species (g) respectively. Corrosion current densities were obtained by the extrapolation of the current–potential lines to the corresponding corrosion potentials. However, the corrosion rates were calculated based on the assumption that the whole surface of steel is attacked by corrosion and no local corrosion pits is observed.

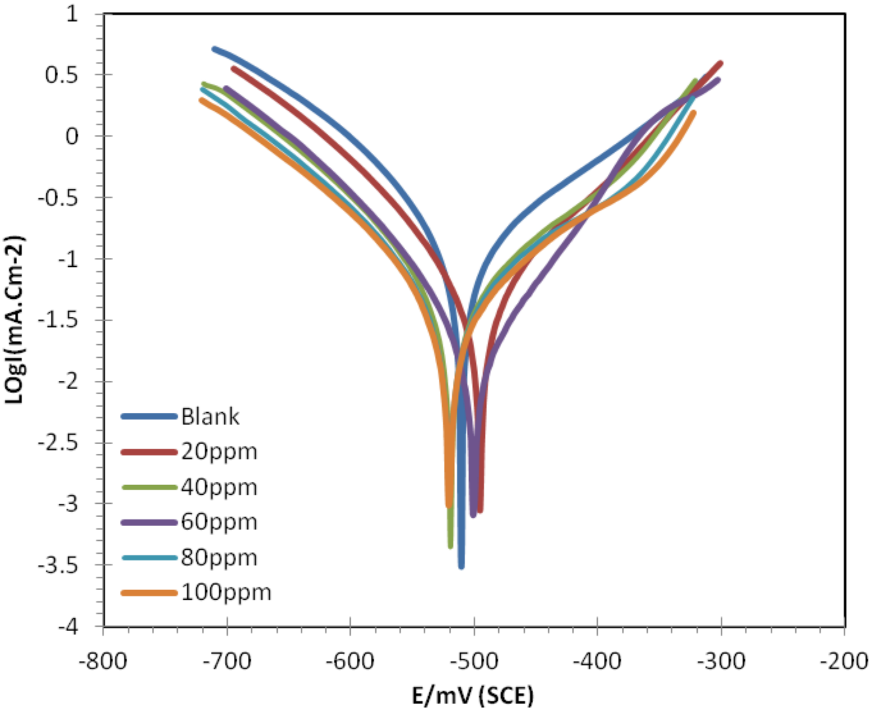

Figure 4. Polarization curves of carbon steel immersed in 1M HCl containing different concentrations of inhibitor LP1.

It is obvious from Figures 4-6 that, the addition of surfactants to the corrosive solution causes the anodic dissolution of iron to reduce and to retards cathodic hydrogen evolution reactions as would be expected. This may be ascribed to the adsorption of the inhibitor molecules over the steel surface. Also, the utilization of the prepared cationic surfactants does not remarkably shift the corrosion potential (E_{corr}), while the anodic and cathodic Tafel slopes changed with the increase of the molecular weight of the prepared surfactants. The increase of molecular weight leads to the increase of hetero-atoms (N and S atoms) which increase the adsorbed atoms on the steel surface. Therefore, these inhibitors can be classified as mixed type inhibitors.

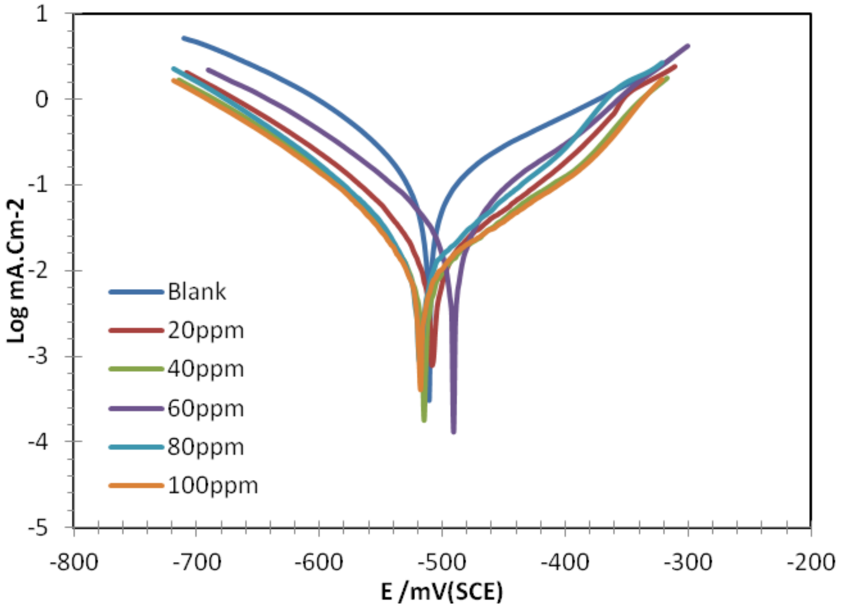

Figure 5. Polarization curves of carbon steel immersed in 1M HCl containing different concentrations of inhibitor LP2.

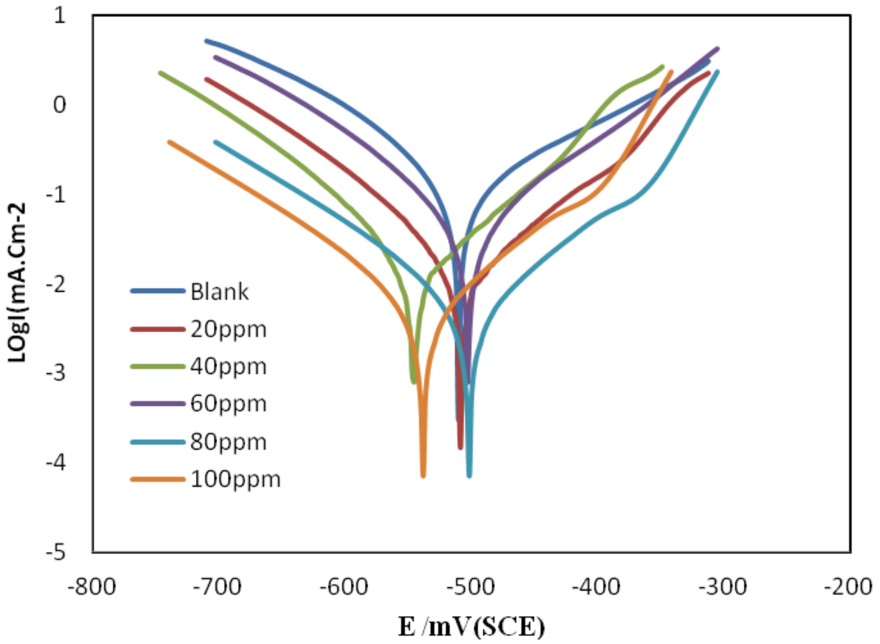

Figure 6. Polarization curves of carbon steel immersed in 1M HCl containing different concentrations of inhibitor LP3.

Table 2. Parameters of potentiodynamic polarization of carbon steel electrode in immersed 1M HCl containing various concentrations of inhibitors at 303 K.

Inhibitor	**Concentration (ppm)**	**E_{corr}, mV**	**I_{corr}, mA/Cm**	**β_a, mV/dec**	**β_c, mV/dec**	**θ**	***I*(%)**
Blank	0	-510	0.28	208	-152	-	-
LP1	**20**	-495	0.11	129	-131	0.59	60
	40	-495	0.11	129	-131	0.59	60
	60	-518	0.097	208	-133	0.66	67
	80	-502	0.08	120	-135	0.71	71
	100	-520	0.07	211	-127	0.75	75
LP2	**20**	-507	0.063	117.5	-127	0.78	78
	40	-508	0.056	122	-129	0.79	80
	60	-504	0.045	131	-135	0.84	84
	80	-508	0.030	152	-197	0.89	89
	100	-512	0.027	143	-143	0.90	90
LP3	**20**	-493	0.051	197	-102	0.82	82
	40	-517	0.035	119	-121	0.87	87
	60	-512	0.025	118	-120	0.91	91
	80	-489	0.015	97	-112	0.95	95
	100	-508	0.007	121	-118	0.97	97

The increasing of hetero-atoms per each molecule leads to the increases in the surface coverage of the inhibitor and hence increasing the adsorption onto the steel surface. [22]. The parallel cathodic Tafel lines suggested that, the addition of inhibitors to 1M HCl solution does not modify the hydrogen evolution mechanism and the reduction of H^+ ions at the steel surface which occurs mainly through a charge transfer mechanism.[23-24]. According to (I%) values represented in Table 2, the inhibitive performance of the studied samples can be given in the following order: LP1< LP2<LP3 with percentages values 75, 90 and 97%, respectively.

3.2.3. Electrochemical impedance spectroscopy (EIS)

Nyquist curves of the tested steel/1M HCl interface in the presence and absence of different concentrations of the prepared inhibitors at 303K was investigated. From Figures 7-9, it is clear that, Nyquist plots of steel in inhibited and uninhibited solutions show a semicircular shape. In spite of the appearance of Nyquist curves remained the same, their diameter increased after the addition of inhibitors to the corrosive solution [25]. This increase was more pronounced with increasing the molecular weight of the tested inhibitors. The adsorption of surfactant molecules on the metal surface was increased by increasing heteroatoms per molecule [26].

The electrochemical parameters estimated from Nyquist curves are determined and listed in Table 3.

The values of R_{ct} were detected by subtracting the high frequency impedance from the low frequency one as follow [27]:

$$R_{ct} = \acute{Z}_{re}\ (at\ low\ frequency) - \acute{Z}_{re}\ (at\ high\ frequency) \qquad \textbf{[4]}$$

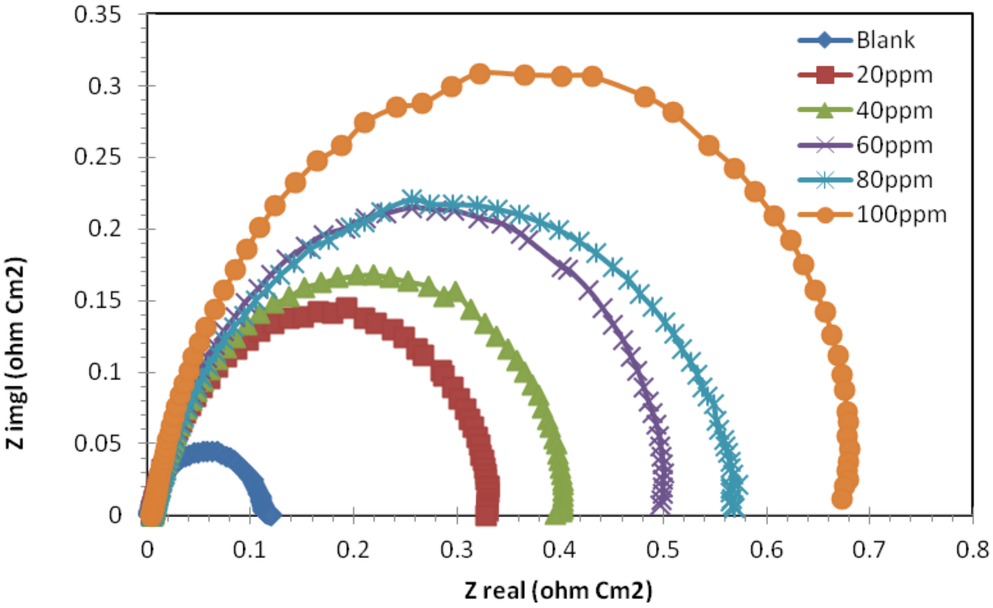

Figure 7. Nyquist plots for the carbon steel immersed in 1M HCl in absence and presence of different concentrations of inhibitor LP1.

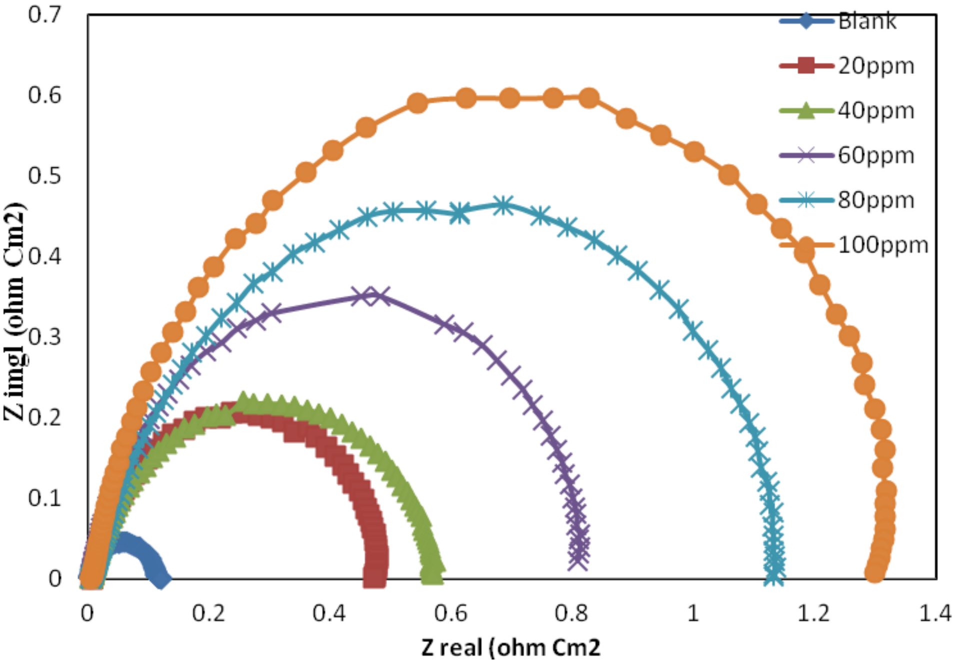

Figure 8. Nyquist plots for the carbon steel immersed in 1M HCl in absence and presence of different concentrations of inhibitor LP2.

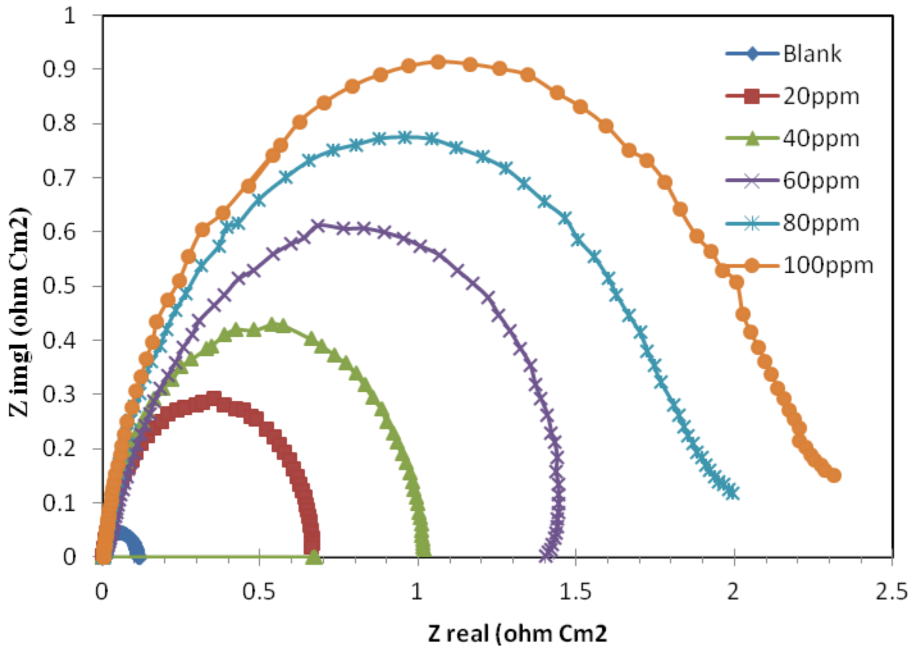

Figure 9. Nyquist plots for the carbon steel immersed in 1M HCl in absence and presence of different concentrations of inhibitor LP3.

Table 3. Impedance measurements and inhibition efficiencies for carbon steel in 1M HCl containing different concentrations of inhibitors at 303 K.

Inhibitor	**Concentration (ppm)**	**R_{ct} Ωm^2**	**R_s Ωm^2**	**C_{dl} μF cm^{-2}**	***I*(%)**
Blank	0	114.2	1.855	69.66	-
LP1	20	307	0.2843	25.91	62.8
	40	322.1	0.6465	24.70	64.5
	60	394	0.7649	20.17	71.03
	80	460.6	0.7325	17.27	75.2
	100	486.5	0.831	16.35	76.52
LP2	**20**	465	0.88	17.12	75.5
	40	570.1	0.60	13.95	79.97
	60	799.7	0.74	9.45	85.72
	80	1135	1.16	7.00	89.93
	100	1303	1.22	6.1	91.23
LP3	**20**	665.1	0.46	11.16	82.3
	40	1022	0.35	6.66	88.8
	60	1434	0.19	5.547	92
	80	1951	0.27	4.077	94.1
	100	2274	0.44	3.49	94.9

The electrochemical double layer capacitance C_{dl} values were calculated at the frequency f_{max}, at which the imaginary component of the impedance is maximal ($-Z_{max}$) by the following equation [28]:

$$C_{dl} = \frac{1}{2\pi f_{max} R_{ct}} \qquad [5]$$

The percentage inhibition efficiency (I %) was determined from the values of R_{ct} according to the following equation [29]:

$$I = \left(\frac{R_{ct(inh)} - R_{ct(uninh)}}{R_{ct(uninh)}}\right) \times 100 \qquad [6]$$

where $R_{ct(inh)}$ and $R_{ct(uninh)}$ are the values of the charge transfer resistance in the presence and absence of the inhibitor, respectively.

Various electrochemical parameters calculated from Nyquist plots are shown in Figures 7-9 and listed in Table 3. It is clear that, the charge-transfer resistance of the modified electrodes is larger than that of the carbon steel electrode, which indicates that the self-assembled films can protect iron from corrosion. Also, the values of both R_{ct} and I % are found to increase by increasing the inhibitor concentration, while the values of C_{dl} decreased. This behavior can be attributed to the decrease in the dielectric constant and/or an increase in the thickness of the electrical double layer, supposing that the inhibitor molecules act by adsorption mechanism at carbon steel/hydrochloric acid solution interface [30]. Thus, the change in C_{dl} values would be a result of the gradual replacement of water molecules by the organic molecules adsorbed on the metal surface and caused the extent of metal dissolution decrease [31].

3.2.4. Weight loss measurements

The corrosion rate (*k*) of steel specimens immersed in 1M HCl solution for 24 hours with and without various concentrations of the prepared surfactants was estimated and illustrated in Table 4. Also, the corrosion rate, *k* (mg cm^{-2} hr^{-1}), surface coverage (θ) and inhibition efficiency *I* (%) of each sample were calculated as follows [32]:

$$k = \frac{\Delta W}{S_t} \qquad \textbf{[7]}$$

$$\theta = \frac{A_{uninh} - A_{inh}}{A_{uninh}} \qquad \textbf{[8]}$$

$$I = \frac{A_{uninh} - A_{inh}}{A_{uninh}} \times 100 \qquad \textbf{[9]}$$

where; ΔW is the average weight loss of three parallel carbon steel sheets (mg), *S* is the total surface area of the specimens (cm^2), *t* is the immersion time (h), and A_{uninh} and A_{inh} are the corrosion rates in the absence and presence of inhibitor, respectively [24]. It was clear from Table 4 that, the inhibition performance (*I*) increased with the decrease of the corrosion rate (*k*) and the increase of the inhibitors concentration. This may be due to the adsorption behavior of the surfactant molecules on the metal surface [17]. Figure 10 shows the variation of (*I%*) and inhibitor concentrations in 1M HCl solution at 303 K and the results indicate the maximum (*I*) values of (100 ppm) of the tested inhibitors LP1, LP2 and LP3 were found to be 77.69, 90.33 and 95.16 %, respectively. This may be due to the increase of (*I*), which is affected by the increasing of molecular weight of the polymeric surfactant molecules. This mean that, the increase in the molecular weight of the inhibitor raise its ability to cover a large surface area of the metal surface [33]. However, the higher inhibition efficiency of LP3 may be according to its high molecular size which ensures its great coverage of the metallic surface and consequently, raise its adsorption rate on this surface [34]. Finally, it was found from EIS and the potentiodynamic polarization measurements data that the obtained results from the weight loss measurements were compatible with them.

Table 4. Gravimetric results of carbon steel after 24 hour of immersion in 1 M HCl without and with various concentrations of the prepared inhibitors at 303 K.

Inhibitor	**Concentration (ppm)**	**k(mg cm^{-2} hr^{-1})**	**θ**	**I(%)**
Blank	0	45.69	-	-
LP1	**20**	17.33	0.62	62.08
	40	16.31	0.64	64.31
	60	15.12	0.68	68
	80	12.23	0.73	73.23
	100	9.9	0.77	77.69
LP2	**20**	10.12	0.73	73.23
	40	8.28	0.77	77.69
	60	4.72	0.84	84.75
	80	3.45	0.88	88.84
	100	3.96	0.90	90.33
LP3	**20**	7.09	0.81	81.78
	40	5.64	0.84	84.75
	60	2.42	0.92	92.19
	80	2.19	0.92	92.93
	100	1.5	0.95	95.16

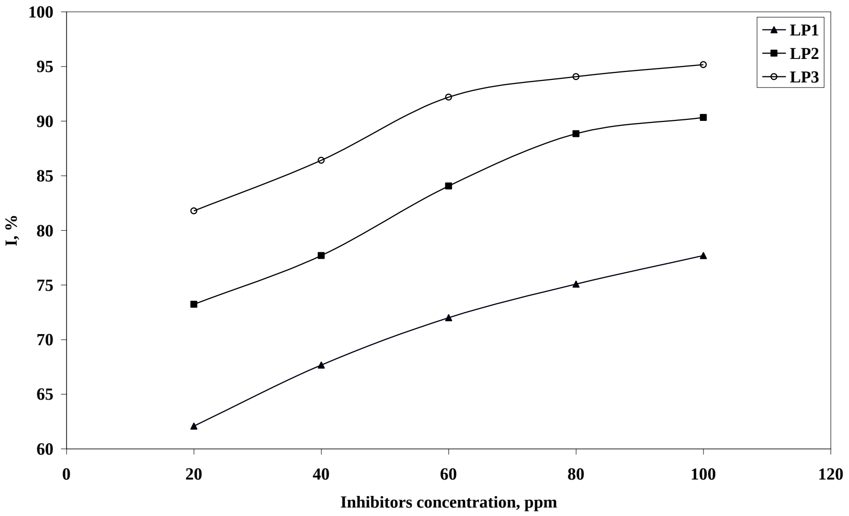

Figure 10. Effect of inhibitors concentration (ppm) on inhibition efficiency (I%) after 24 hour immersion in 1 M HCl at 303 K.

3.3. Adsorption isotherm and standard adsorption free energy

Corrosion inhibition by organic compounds is mainly due to their ability to be adsorbed onto a metal surface to form a protective film. The adsorption of organic inhibitors at the metal/solution interface takes place through the replacement of water molecules by organic inhibitor molecules according to following process [35]: -

$$org_{(sol)} + x\,H_2O_{(ads)} \rightarrow org_{(sol)} + xH_2O_{(ads)} \qquad [10]$$

where $Org_{(sol)}$ $Org_{(ads)}$ and x are organic molecules in the solution, adsorbed molecules on the metal surface and the number of water molecules replaced by the organic molecules respectively. The mode of adsorption can be obtained from the adsorption isotherm through the inhibitor interaction behaviores on the metal surface. [36]. The investigated surfactants in 1M HCl solution were tested with several adsorption isotherms to best fit the adsorption process using weight loss data. [37]. Surface coverage values (θ) at different concentrations of LP1, LP2 and LP3 and at 303 K and after 4 hours of immersion are calculated from the following equation: -

$$\frac{C_i}{\theta} = \frac{1}{k_{ads}} + C_i \qquad [11]$$

where C_i is the concentration of tested polymer and K_{ads} is the adsorptive equilibrium constant. Langmuir's isotherm assumes that, there is no interaction between the adsorbed molecules, the energy of adsorption is independent on the θ, the solid surface contains a fixed number of adsorption sites, and each site holds one adsorbed species. C_i/θ against C_i curves yield straight lines as shown in Figure 11, and the linear regression parameters are listed in Table 5. Both linear correlation coefficient (r) and the slope are very close to 1, indicating the adsorption of the tested surfactants on steel surface obeys Langmuir adsorption isotherm. The adsorptive equilibrium constant (K_{ads}) can be estimated from reciprocal of intercept of C_i/θ–C_i isotherm. K_{ads} is related to the standard free energy of adsorption (ΔG^o_{ads}) as shown from the following equation [38]:

$$K_{ads} = \frac{1}{55.5} \exp\left(\frac{-\Delta G^\circ_{ads}}{RT}\right) \qquad [12]$$

where R is the gas constant (8.314 J mol^{-1} K^{-1}), T is the absolute temperature (K), and the value 55.5 is the concentration of water in solution expressed in molar. From the results presented in Table 5, the high values of K_{ads} and negative values of ΔG°_{ads} suggested that, surfactant molecules strongly adsorbed on the steel surface. Generally, values of ΔG°_{ads} up to -20 kJ mol^{-1} are consistent with the electrostatic interaction between the charged molecules and the charged metal (physical adsorption), while those of more negative than -40 kJ mol^{-1} involve sharing or transfering of electrons from the tested molecules to the metal surface forming a coordinate type of bond (chemisorption) [39]. ΔG°_{ads} values for the three studied compounds being less than (-40 kJ mol^{-1}) and greater than (-20 kJ mol^{-1}) indicating physicochemical adsorption bond (physical and chemical adsorption) on the metal surface this may be according to electrostatic interaction and there may be some other interactions [40].

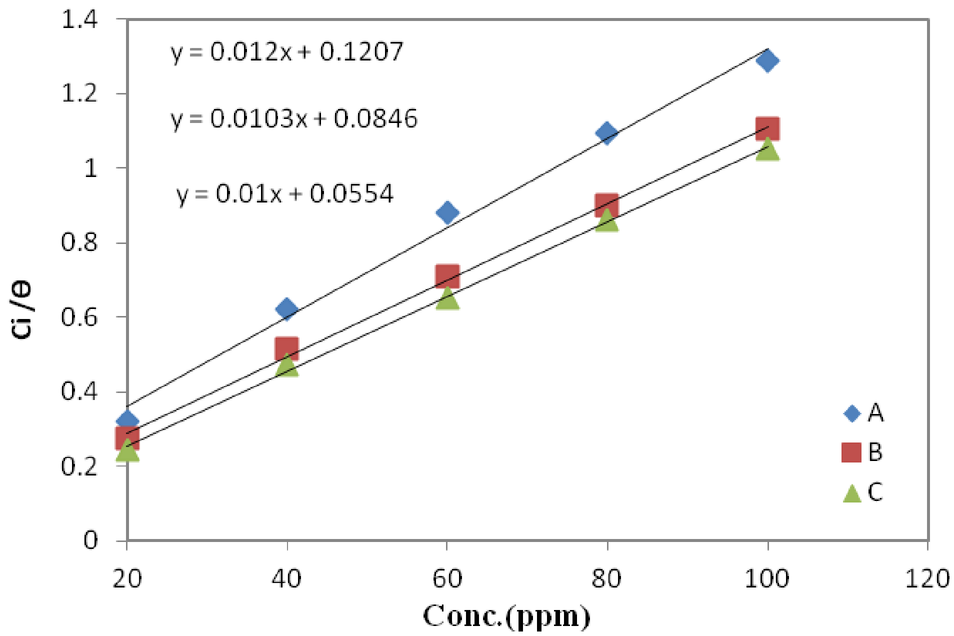

Figure 11. Adsorption plots of steel in 1 M HCl solution containing the prepared inhibitors at 303 K.

Table 5. Adsorption equilibrium constant (K_{ads}) and standard free energy of adsorption (ΔG^o) of the inhibitors for steel in 1 M HCl solution at 303 K.

inhibitor	Linear correlation coefficient (r)	slope	K_{ads} (M^{-1})	ΔG^o_{ads} (kJ mol^{-1})
LP1	0.998	0.012	459817.7	-32.846
LP2	0.998	0.01	656028.4	-33.7413
LP3	0.998	0.01	1001805	-34.8078

3.3.1. Scanning electron microscopy (SEM)

Figure 12(1) shows the SEM image of the polishing steel surface whereas Figure 12(2) shows the image of untreated steel after immersion in 1M HCl for 24 hours (blank). The SEM images of treated steel samples with 100ppm of LP1, LP2 and LP3 surfactants in 1M HCl for 24 hours are shown in Figures 12(3-5) respectively. It was clear from the images that, the carbon steel surface is highly corroded in the absence of the inhibitor. Whereas smoother surface is seen in the presence of the inhibitor especially in case of LP3 sample Figure 12(5), which gave a similar surface to that in Figure 12(1) for the polished surface. These results indicated that, the surfactant molecules inhibit the dissolution of steel by formation a protective film on the steel surface [23].

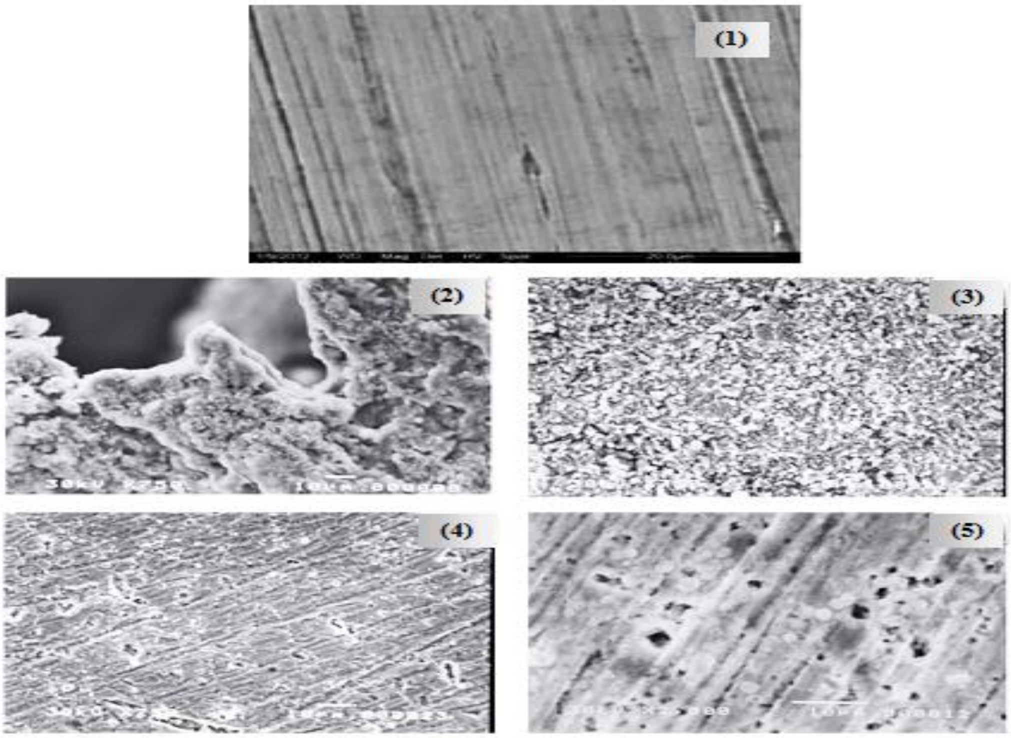

Figure 12. SEM micrographs of steel samples: (**1**) only polished surface, (**2**) after 24 h of immersion in 1 M HCl solution, (**3**) after 24 hour of immersion in 1 M HCl solution in the presence of 100 ppm of LP1, (**4**) in the presence of LP2 and (**5**) in the presence of LP3.

3.3.2. Quantum chemistry calculations

The effectiveness of the inhibitor can be related to its spatial molecular structure, as well as their molecular electronic structure. The quantum chemical methods study the relationship between the organic molecular structure and the inhibition effect.

From Figures 13-15 and Table 6, it was obvious that, the higher the E_{HOMO} energy (E_H) of the inhibitor, the ease of offering electrons to the unoccupied d orbital of carbon steel increased and the inhibition performance of the prepared polymer for carbon steel in 1M HCl solution increase. The lower the E_{LUMO} energy (E_L), the easier the acceptance of electrons of the d- orbital of carbon steel and the higher the inhibition efficiency of the tested compounds for carbon steel. Also, the ΔE decrease when the surfactants inhibition efficiency increased indicating the more stability of the adsorbed molecules. Thus, the interactions between the inhibitor and the metal surface are probably physical adsorption bond [41]. Inspection of data listed in Table 6, the dipole moment (μ) of the inhibitors changed regularly, which proved that, the adsorption might have a risen from the intermolecular electrostatic force. The lowest value of dipole moment with maximum inhibition efficiency was observed with LP3 due to the increase of accumulation of inhibitor molecules on the metallic surface [42]. It is worth noted from Table 7, that $\mu_{\text{inhibitor}}$ of LP3 (3.065 eV mol^{-1}) has the highest probability to form a coordinating bond by accepting an electron from the metal surface ($\mu_{Fe=}$ 7 eV mol^{-1}). Also, the effect of global hardness ($\eta_{\text{inhibitor}}$) and softness (σ, eV^{-1}) on the inhibitors efficiency were investigated. From Table 7, it was observed that, the softness (σ) increases from 0.169 to 0.198(eV^{-1}) for LP1 and LP3, respectively. This means that, the adsorption of the tested inhibitors upon the metal surface increases with increasing the value of (σ), whereas, the increasing of repeating unit of (LP3) leads to an increase in the number of electrons transferring from the inhibitor to the metal surface, thus a strong protective film was formed on the metal surface [18,43]. Finally LP3 inhibitor has the highest inhibition efficiency because it has the lowest energy gap (Δ*E*) values, and it is the most capable one of offering electrons.

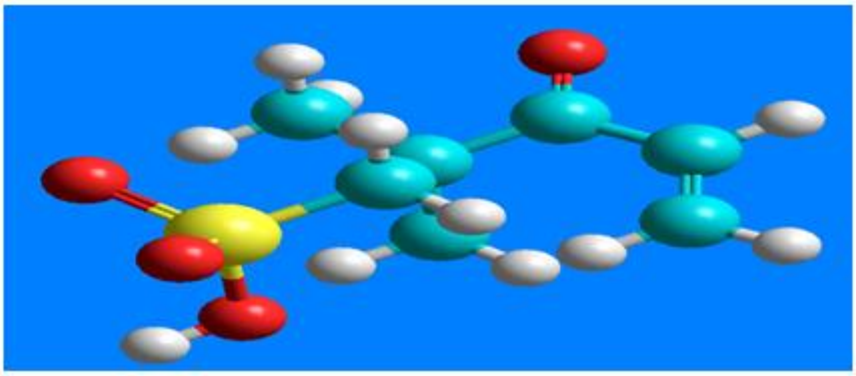

Figure 13. Equilibrium structure of the LP3

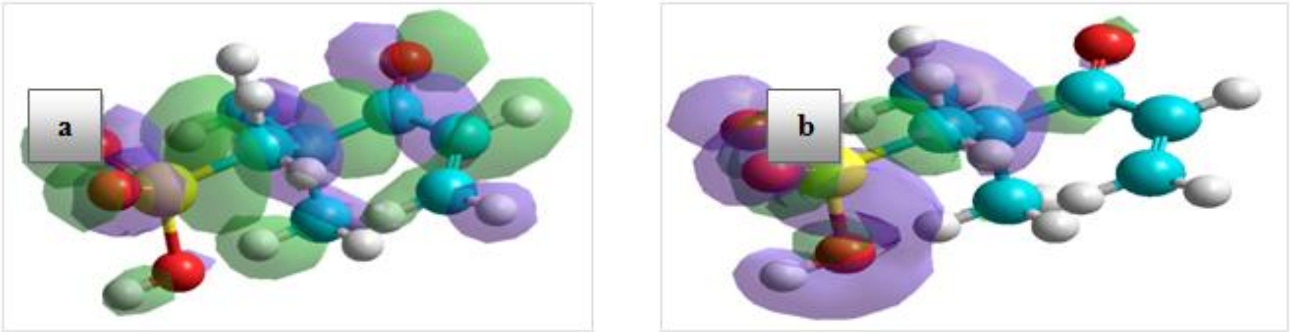

Figure 14. Frontier molecule orbital density distributions of LP3 (a) HOMO and (b) LUMO.

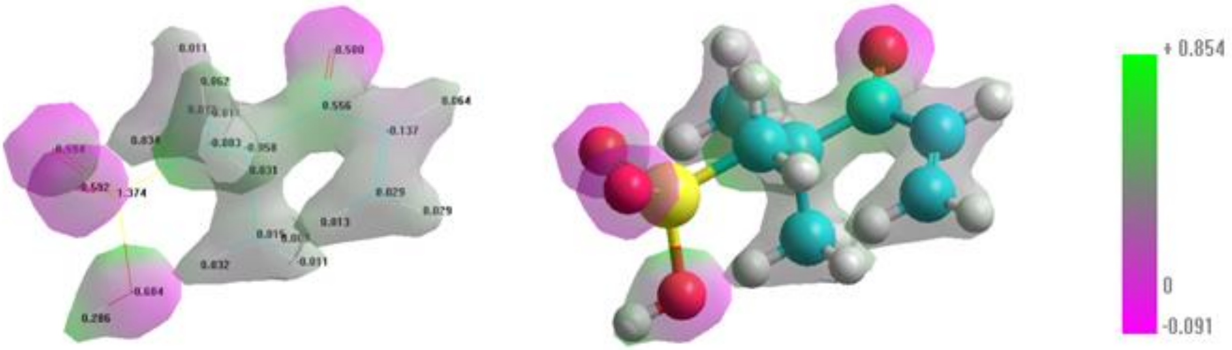

Figure 15. Molecular electrostatic potential map of LP3.

Table 6. Quantum chemical parameters of the investigated inhibitors

Inhibitor	**E_{HOMO}(E_H), eV**	**E_{LUMO}(E_L), eV**	**ΔE, eV**	**μ, debye**	**Log P**	**Polarizability (Å3)**	**Hydration energy, E_{hydr}, (K Cal. mol^{-1})**	**Surface area, A, (nm^2)**	**Total energy, E_T, (eV)**
LP1	-9.64	2.156	11.7	5.2	2.1	18.16	-23.22	654	-34712
LP2	-9.36	2.03	11.39	3.37	3.42	24.76	-8.16	550.4	-75265
LP3	-8.1	1.97	10.07	3.21	4.48	31.03	-9.41	676.87	-88176

Table 7. Other calculated quantum chemical parameters of the investigated inhibitors

Inhibitor	**Ionization potential, I_p (eV)**	**Electron affinity, E_A(eV)**	**Electron negativity of the inhibitor, $i_{inhibitor}$ (eV mol^{-1})**	**Electronic chemical potential of the inhibitor, $\mu_{inhibitor}$ (eV mol^{-1})**	**Global hardnes, $\eta_{inhibitor} = \Delta E/2$ (eV mol^{-1})**	**Sotness, $\sigma=1/\eta_{inhibitor}$ (eV^{-1})**
LP1	9.64	-2.156	3.7	-3.74	5.89	0.169
LP2	9.36	-2.03	3.665	-3.665	5.695	0.175
LP3	8.1	-1.97	3.065	-3.065	5.035	0.198

The theoretical values of absolute electronegativity (χFe), the absolute hardness (η_{Fe}) and the electronic chemical potential (μ_{Fe}) of iron are 7, 0 and -7 eV/mol respectively.

4. CONCLUSION

(2-acrylamido-2-methylpropane sulfonic acid / lauryl acrylate) three new anionic polymeric surfactants were prepared and and evaluated as corrosion inhibitors for carbon steel alloy in acidic solution. The data showed that the efficiency of the prepared polymeric surfactant is mainly depends on the molecular weight and the (R1/R2) ratio per molecules. Also, the potentiodynamic polarization plots indicate that all inhibitors behaved as mixed type inhibitor by inhibiting both anodic metal dissolution and cathodic hydrogen evolution reactions. The weight loss, polarization and Impedance measurements results are compatible and showed that all the three polymeric surfactants exhibit a good inhibition performance. Finally LP3 inhibitor has the highest inhibition efficiency (97%) because it has the lowest energy gap (ΔE) values, and it is the most capable one of offering electrons.

Reference

1. A.A. Farag, M.R. Noor El-Din, *Corros. Sci.,* 64 (2012) 174.
2. H.. Choi, Y. K. Song, K. Y. Kim, J. M. Park, *Surf. Coat. Technol.,* 206 (2012) 2354.
3. A.M. Atta, O. E. El-Azabawy, H.S. Ismail, M.A. Hegazy, *Corros. Sci.,* 53 (2011) 1680.
4. M.A. Hegazy, A.S. El-Tabei, A.H. Bedair, M.A Sadeq , *Corros. Sci.,* 54(2012)219.
5. M.A. Hegazy, M.F. Zaky, *Corros. Sci.,* 52 (2010) 1333.
6. G. Banerjee, S.N. Malhotra, *Corrosion,* 48 (1992) 10.
7. A.K. Maayta, M.B. Bitar, M.M. Al-Abdallah, *Brit. Corros. J.,* 36 (2001) 133.
8. S.S. Abd El Rehim, H.H. Hassaan, M.A. Amin, *Mater. Chem. Phys.,* 70 (2001) 64.
9. V. Branzoi, F. Golgovici, F. Branzoi, *Mater. Chem. Phys.,* 78 (2002) 122.
10. N.O. Eddy, U.J. Ibok, E.E. Ebenso, A .El Nemr, H.E. El Ashry, *J. Mol. Model.,* 15(2009) 1085.

11. R. K. Farag, *International Journal of Polymeric Materials*, 57(2008),189.
12. A.M.Al-sabagh, A.M. Sharaky, M.R. Noor El-Din and K. M. Hussein, *Tenside Surfactant and Detergent*, 52 (2015) 88.
13. M .S. Alam, B.M. Asit, *J. Mol. Liquids*, 168(2012)75.
14. O.Y. Ayse, S. Ramazan, K. Gulfeza, *Mater. Chem. Phys.*, 131(2012) 615.
15. M. R. Noor El-Din, *Journal of Dispersion Science and Technology*, 301027.
16. M. R. Noor El-Din, E. A. Khamis, *J. Surfact. Deterg.,* 17(2014) 795.
17. L.M. Harwood, T.D.W Claridge, *Introduction to organic spectroscopy*– oxford Chemistry Primers Series, 43. San Val -Incorporated, UK, (1996) pp 22–32
18. G.E. Badr, *Corros. Sci.*, 51 (2009) 2529.
19. J. M. Corkill, J. T. Goodman, and S. P. Harrold, *Trans. Faraday Soc.*, 60 (1964) 202.
20. A. M. Al-Sabagh, E. M. S. Azzam, and M. R. Noor El Din, *Journal of Dispersion Science and Technology*, 30(2009)260.
21. M.R. Noor El-Din, A.M. Al-Sabagh, M.A. Hegazy, *J. Dispers. Sci. Technol*., 33(2012) 1.
22. M.A. Hegazy, M.F. Zaky, *Corros. Sci.,* 52(2010) 1333.
23. R. Solmaz, G. Kardas, M.C. Ulha, B. Yazici, M. Erbil, *Electrochim. Acta*, 53 (2008) 5941.
24. N.A. Negm, A. F. El Farargy, E. A. Badr, M. F. Zaki, *Journal of Applied Chemistry*, 7 (2014) 13
25. M. Behpour, S.M. Ghoreishi, N. Soltani, M. Salavati-Niasari, *Corros. Sci.,* 51 (2009) 1073.
26. N.A. Negm, M.F. Zaki, *Colloids Surf.*, A 322 (2008) 97.
27. A.M. Abdel-Gaber, M.S. Masoud, E.A. Khalil, *Corros. Sci.*, 51 (2009) 3021.
28. M. Behpour, S.M. Ghoreishi, A. Gandomi-Niasar, N. Soltani, M. Salavati-Niasari, *J. Mater. Sci.,* 44 (2009) 2444.
29. I. Ahamad, M.A. Quraishi, *Corros. Sci.,* 51 (2009) 2006.
30. M.A. Hegazy, M. Abdallah, H. Ahmed, *Corros. Sci.,* 52 (2010) 2897.
31. M.A. Hegazy, *Corros. Sci*,. 51 (2009) 2610–2618.
32. H.H. Hassan, E. Abdelghani, M.A. Amin, *Electrochim. Acta*, 52 (2007) 6359.
33. K.Y. Dileep, M.A. Quraishi, B. Maiti, *Corros. Sci*., 55 (2012) 254.
34. M.A. Migahed, H.M. Mohamed, A.M. Al-Sabagh, *Materials chemistry and physics,* 80 (2003) 169.
35. L.i. Xianghong, S. Deng, H. Fu, L.i. Taohong , *Electrochim. Acta,* 54 (2009) 4089.
36. D.Q. Zhang, Q. R. Cai, X. M. He, L.i-Xin Gao, G.S. Kim, *Mater. Chem. Phys.*, 114 (2009) 612.
37. H. Keles, M. Keles, I. Dehri, O. Serindag, *Mater. Chem. Phys.*, 112 (2008) 173.
38. R. Solmaza, E. Altunbas, G. Kardas, *Mater. Chem. Phys.,* 125 (2011) 796.
39. R. Solmaz, G. Kardas, B. Yazıcı, M. Erbil, *Colloids Surf., A* 312 (2008) 7.
40. H. Keles, M. Keles, I. Dehri, O. Serindag, *Colloids Surf., A* 320 (2008) 138.
41. N.O. Eddy, U.J. Ibok, E.E. Ebenso, A .El Nemr, H.E. El Ashry, *J. Mol. Model.,* 15(2009)1085.
42. Y .Ying, L .Weihua, L. Lankun L, Baorong, *Electrochim. Acta*, 53(2008) 5953.
43. A. M. Atta , G. A. El-Mahdy, H. A. Allohedan and Sh. M. El-Saeed, *International Journal of electrochemical science,* 10 (2015) 8 .